Kinetics of Antibody-Dependent Binding of Haptenated Phospholipid Vesicles to a Macrophage-Related Cell Line†

J. Todd Lewis,‡ Dean G. Hafeman, and Harden M. McConnell*

ABSTRACT: We have measured the kinetics of specific antibody-dependent binding (and phagocytosis) of haptenated lipid vesicles to RAW264 macrophages as a function of antibody density on the vesicle surface and lipid composition of the vesicles. Fluid vesicles (dimyristoylphosphatidylcholine at 37 °C) bind much more rapidly to macrophages than do solid vesicles (dipalmitoylphosphatidylcholine at 37 °C). Inclusion of cholesterol in the dipalmitoylphosphatidylcholine vesicle membrane results in a large enhancement in binding rate, whereas inclusion of cholesterol in the dimyristoylphosphatidylcholine membrane has a much smaller effect (37 °C). The rate of vesicle binding also depends on the antibody density on the vesicle surface. In the presence of cytochalasin B, vesicle phagocytosis is completely inhibited in the case of dimyristoylphosphatidylcholine vesicles and partially inhibited in the case of dipalmitoylphosphatidylcholine vesicles. An analysis of the vesicle to macrophage binding kinetics has been made, leading to the conclusion that receptors are internalized along with vesicles during phagocytosis, and these receptors are not replaced during the time of the experiment. The analysis of the data shows an exponential relationship between vesicle binding (and phagocytosis) and receptor loss, such that vesicles binding at later times deplete the macrophage of fewer receptors than do vesicles binding at earlier times. The difference in the rate of binding of dimyristoylphosphatidylcholine and dipalmitoylphosphatidylcholine vesicles to the macrophages can be accounted for in terms of the difference in the lateral diffusion coefficients of antibodies bound to these vesicle surfaces. The addition of cholesterol to the dipalmitoylphosphatidylcholine membrane enhances this diffusion coefficient. The above considerations are incorporated into a simple kinetic model for the binding rates of vesicles to macrophages.

The interaction of a phagocytic cell with an antibody-coated target cell can be thought of as an example of cell–cell recognition and triggering. Antigens on the target cell are first "recognized" by specific antibodies; the Fc stems of the bound antibodies are "recognized" by the Fc receptors of the phagocytic cell, which in turn triggers phagocytosis or cytolysis of the target cell. In the present work we have simplified this "model" of cell–cell recognition even further by using haptenated lipid vesicles in place of the target cell, since the physical and chemical properties of such vesicles can be controlled with considerable precision. By varying these physical and chemical properties and by studying the phagocytic activity, one can hope to understand better the molecular events that are typically involved in cell–cell recognition. We have investigated the relation between molecular motion in the vesicle target membranes and the kinetics of vesicle binding and/or phagocytosis by RAW264 macrophages. We have also attempted to provide a quantitative analysis of the kinetic results. Other studies of specific antibody-dependent interactions between cells of the immune system and haptenated lipid membranes include work by Geiger & Schreiber (1979), Henkart & Blumenthal (1975), and Hafeman et al. (1979).

The present study has been carried out in parallel with studies of the kinetics of specific antibody-dependent activation of the first component of complement by similar lipid target membranes. The results we have obtained for specific antibody-dependent binding of haptenated lipid target membranes are strikingly similar to those observed for the specific antibody-dependent activation of the first component of complement, in that "fluid" target membranes are much more effective than "solid" target membranes (Esser et al., 1979; Parce et al., 1980). Here "fluid" and "solid" refer to lipid membranes where the lateral diffusion coefficients of lipid haptens as well as antibody bound to these haptens are on the order of $\geq 10^{-8}$ and $\leq 10^{-10}$ cm^2/s, respectively (Smith et al., 1979). These conclusions evidently apply only to certain steps in target membrane recognition and triggering in the case of RAW264 macrophages, since, as discussed in the accompanying paper (Hafeman et al., 1980), some biochemical events (oxygen consumption and 1-*C*-glucose oxidation) are much more extensive for the solid target membranes than for the fluid target membranes. Thus the biophysical and biochemical consequences of a change from the solid to fluid state of a target membrane need not always be in the same direction. For recent reviews on endocytosis and macrophages, see Stossel (1977), Ralph (1980), and a monograph edited by Baram et al. (1979).

Materials and Methods

Hapten and Lipids. The dipalmitoylphospholipid nitroxide spin-label hapten (I) was synthesized by D. Torney according

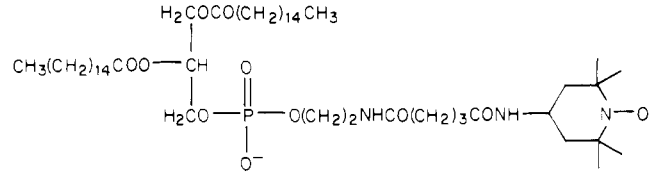

I

to a modification of Brûlet's original synthesis (Brûlet & McConnell, 1977) developed by L. Smith and D. Torney (unpublished experiments).

The fluorescent phospholipid probe, *N*-(4-nitrobenzo-2-oxa-1,3-diazolyl)phosphatidylethanolamine (NBD-PE),[1] pre-

† From the John Stauffer Laboratory for Physical Chemistry, Stanford University, Stanford, California 94305. *Received March 6, 1980.* This work was funded by National Institutes of Health Grant No. 5R01 AI13587. J.T.L. has received support from National Institutes of Health Training Grant GM07276-05. D.G.H. has been supported by a National Institutes of Health postdoctoral fellowship.

‡ Present address: Immunology Branch, National Cancer Institute, National Institutes of Health, Bethesda, MD 20014.

0006-2960/80/0419-5376$01.00/0

pared from egg lecithin, was purchased from Avanti Biochemicals, Birmingham, AL. DMPC and DPPC, Grade A, were purchased from Calbiochem and stored as 10 μmol/mL stock solutions in methanol at −20 °C. Cholesterol, Sigma Grade, was purchased from Sigma Chemical Co. and stored as a 1 μmol/mL stock solution in ethanol under argon at −20 °C. [1-^{14}C]DPPE was purchased from Applied Science Laboratories, Inc., State College, PA. All lipids were used without further purification unless otherwise noted.

Phospholipid Vesicles. Large unilamellar vesicles were prepared by a modification of the ether injection method of Deamer & Bangham (1976). A lipid mixture of some selected composition, 10 μmol total, with 1.4 μCi of [^{14}C]DPPE, was dried from stock solutions under partial vacuum at room temperature on a Büchi rotary evaporator and redissolved in 5 mL of methanol/diethyl ether (1:4 v/v). An aliquot of this solution was mixed with 10 mL of ACS counting solution (Amersham Corp., Arlington Heights, IL) and a count rate was determined on a Nuclear Chicago liquid scintillation counter. The lipid solution, at room temperature, was injected into 5 mL of PBS, maintained at 62 °C, through a crimped syringe needle (18 gauge) at a rate of 0.25 mL/min. (The syringe needle was crimped so that a fine spray resulted when ether was forced through the needle into air at the injection rate used.) An expansion chamber at the top of the PBS compartment trapped foam produced during the injection process and returned it to the PBS. After injection was complete, the PBS, containing vesicles thus formed, was placed on ice.

Vesicle subpopulations were selected by differential centrifugation at 0 °C in a Lourdes 9RA fixed angle rotor using 15-mL Corning glass centrifuge tubes. A fraction of vesicles which pelleted at 5000 rpm (3000*g*) in 5 min was termed the "large" fraction. The supernatant was centrifuged at 10000 rpm (12000*g*) for 20 min. The pellet of vesicles was collected and termed the "medium" fraction. The supernatant of the above spin was centrifuged at 15000 rpm (27000*g*) for 80 min. The resulting pellet was collected and termed the "small" fraction. All vesicle fractions were resuspended in PBS to a concentration of 0.25 μmol of lipid/mL, using the [^{14}C]DPPE marker to determine the dilution factor.

Increasing cholesterol concentration resulted in fewer vesicles in the large fraction. At or at greater than 15 mol % cholesterol, no significant large fraction was obtained. Light microscopy revealed that the size distribution of vesicles containing >15 mol % cholesterol in the medium fraction was similar to that of pure DPPC vesicles in the large fraction, indicating that the DPPC vesicles have a greater density, due to a greater lipid density and possibly also to a greater number of lamellae for DPPC. The yield of DMPC vesicles in the large fraction was consistently ~60% of the large DPPC yield. See Table I and legend for further description of vesicles.

Multilamellar vesicles (liposomes) were formed by drying a lipid mixture of some selected composition (1 μmol of total lipid) from 10:1 chloroform/methanol (v/v) in a round-bottom flask on a Büchi rotary evaporator flushed with argon under partial vacuum at 37 °C for 15 min. The dried film was hydrated with 1 mL of PBS under argon at 60 °C and swirled by hand to form liposomes of heterogeneous sizes. Cholesterol for cholesterol-containing liposomes was first purified by the method of Humphries & McConnell (1979).

All phospholipid vesicles and liposomes used in this study contained 1 mol % nitroxide spin-label phospholipid hapten, 1 mol % NBD-PE, and varying compositions of DPPC, DMPC, and cholesterol.

Antibodies. Antinitroxide IgG was prepared by immunizing rabbits according to a procedure described by Humphries & McConnell (1976), with the modification that an alum precipitate of 100 μg of spin-labeled keyhole limpet hemocyanin was used in the boosting intravenous injections. The quantity and affinity of antinitroxide antibody varied greatly from rabbit to rabbit, so that it was necessary to identify two individual "high responders" from a population of 10 New Zealand white females.

Affinity purified specific antinitroxide antibody was prepared as described previously (Henry et al., 1978). A protein A purified IgG fraction was prepared as described previously (Esser et al., 1979). A Scatchard analysis as described by Rey & McConnell (1976) was used to determine the specific antinitroxide antibody concentrations in each preparation. The single Fab binding affinity was estimated to be 5×10^6 L/mol.

Unless otherwise noted, the antibody preparations were centrifuged at 20 psi (100000*g*) for 20 min in a Beckman airfuge (to remove antibody aggregates) immediately prior to use.

Macrophages. The RAW264 macrophage-related cell line was a gift of Dr. Peter Ralph. Properties of this cell line have been described in detail elsewhere (Ralph & Nakoinz, 1977). The RAW264 line was cultured and harvested as described by Lewis (1980).

The adherent cells were incubated with PBS, 2 mM EDTA, 0.1% glucose, and 5% (v/v) fetal bovine serum at room temperature for 30 min. At the end of the incubation period, the flask was sealed and shaken vigorously by hand to detach the adherent cells, and the resulting cell suspension was centrifuged at 250*g* for 3 min at 20 °C. The pellet was resuspended to 3.3×10^6 viable cells/mL in cell buffer [2.0 mM $CaCl_2$, 1.5 mM $MgCl_2$, 5.4 mM KCl, 1 mM Na_2HPO_4, 5.6 mM glucose, 120 mM NaCl, and 0.2% bovine serum albumin (Calbiochem, fatty acid poor), pH 7.4]. Cell viability was consistently >85% as estimated by trypan blue exclusion.

Vesicle Binding Assay. Polypropylene vials (1.2 × 5.0 cm, E & K Scientific Products, Inc., Saratoga, CA) were used in the binding assay. (Lipid sticks to polystyrene.) Vesicles (100 μL, 0.020 or 0.025 μmol of total lipid suspended in 0.15 M NaCl) and antibody (previously diluted into 100 μL of cell buffer) were added as physically separate drops in each vial. From 15 to 30 min prior to incubation with macrophages, antibody and vesicles were thoroughly mixed by swirling the vials rapidly. Macrophages (1×10^6) were added to each vial in cell buffer to bring the final volume to 0.5 mL, and the mixtures were incubated at 37 °C in a gyrotary water bath shaker (Model G76, New Brunswick Scientific Co., New Brunswick, NJ) at 170 cycles/min. After the indicated times the vials were removed and chilled in ice water. The content of each tube was layered with a polypropylene pipet tip onto 0.5 mL of 10% Ficoll (Pharmacia, Uppsala, Sweden) in cell buffer in a 1.0-mL polystyrene centrifuge tube (Fischer Scientific), capped, and spun at 500*g* for 20 min. The unbound vesicles at the interface and in the supernatant were drawn off with a Pasteur pipet, and radioactivity was determined by mixing the vesicles with 10 mL of ACS (Amersham Corp., Arlington Heights, IL) and counting in a liquid scintillation counter. The Ficoll precipitate formed in this mixture did not interfere with counting efficiency.

[1] Abbreviations used: DMPC, dimyristoylphosphatidylcholine; DPPC, dipalmitoylphosphatidylcholine; NBD-PE, *N*-(4-nitrobenzo-2-oxa-1,3-diazolyl)phosphatidylethanolamine; PBS, phosphate-buffered saline; EDTA, ethylenediaminetetraacetic acid; Hepes, *N*-2-hydroxyethylpiperazine-*N*′-2-ethanesulfonic acid.

Binding was calculated as

$$\% \text{ binding} = \left[1 - \frac{\text{cpm(experimental)} - \text{cpm(background)}}{\text{cpm(control)} - \text{cpm(background)}}\right] \times 100$$

where the control was either lipid incubated without macrophages or, in the case of kinetic studies, macrophages and lipids mixed and maintained at 0 °C and then centrifuged on the Ficoll step density gradient and counted as described above. Control studies showed that RAW264 macrophages do not bind any of the antibody-coated vesicles while at 0 °C. In experiments designed to measure binding at early times, the macrophage pellet was also counted. In some experiments (cf. Figure 5) macrophages were sonicated in distilled water and ACS was added for counting. In later experiments (not described here in detail) the centrifuge tube containing the Ficoll step gradient was frozen and then cut to separate the pellet from the supernatant. The tip containing the pellet was thawed and then placed in a glass tube cut to fit the scintillation vial, and then 0.4 mL of tissue solubilizer (NCS, Amersham Corp.) was added and maintained at 50 °C for 45 min. Samples were neutralized with acetic acid, and 10 mL of toluene based fluor was added and mixed thoroughly. The scintillation discriminator was carefully set to eliminate counts from chemiluminescence and phosphorescence. This procedure, although time consuming, proved to be highly reproducible. Results obtained by using this method were reproducible to within a few percent and can be accounted for quantitatively by the theoretical treatment given later.

Results

Binding as a Function of Antibody Density on the Vesicle. A measurement of specific antinitroxide rabbit antibody binding to liposomes composed of either DMPC or DPPC and 1 mol % nitroxide spin-label phospholipid hapten (I) has shown that fewer antibodies (by a factor no larger than 2) bind to DPPC liposomes than to DMPC liposomes for densities of antibody on the surface of the liposomes less than a 1:1 antibody/exposed hapten ratio. This difference diminishes as the antibody concentration is lowered. For example, 75 ± 5% of the antibodies are bound to each membrane when the antibody/exposed hapten ratio is 1:81 at 37 °C (Humphries & McConnell, 1980).

When the amount of antibody bound to hapten-containing phospholipid vesicles is approximately the same, more DMPC (fluid at 37 °C) than DPPC (solid at 37 °C) vesicles become associated with the RAW264 macrophages after 1 h of incubation at 37 °C. At an antibody/exposed hapten ratio of 1:625 (antibody surface density = 27/μm^2) 65% of the DMPC vesicles become associated with the macrophages as opposed to 5% of the DPPC vesicles (see Figure 1). [Table I gives values of antibody/exposed hapten ratios, antibody surface densities, and the number of antibodies per vesicle.] Examination of the macrophages with a fluorescence microscope after the 1-h incubation showed that all of the vesicles were phagocytized; the internalized vesicles appeared to retain their shape and size after this period of time. Earlier studies by Lewis & McConnell (1978) indicate loss of vesicle contents when vesicles are phagocytized by macrophages. The presence of 2 μg/mL cytochalasin B diminished the amount of ^{14}C-labeled phospholipid associated with the macrophages only slightly (Figure 1). At an antibody/exposed hapten ratio of 1:25, 2 μg/mL cytochalasin B completely inhibited the phagocytosis (but not binding) of DMPC phospholipid vesicles but only partially inhibited the phagocytosis of DPPC vesicles.

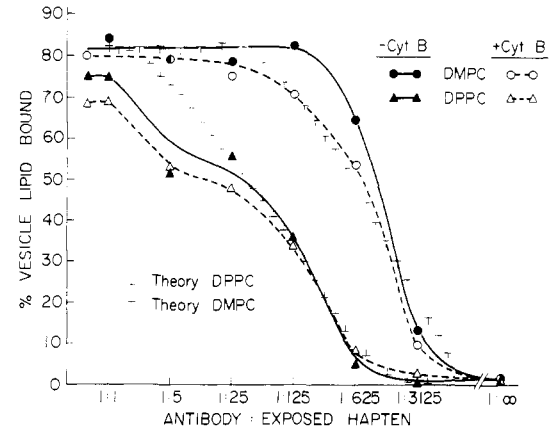

FIGURE 1: Binding of vesicle lipids to RAW264 macrophages as a function of antibody/exposed hapten ratio. Binding was measured after a 1-h incubation as described in the text. The lipids employed were DMPC (fluid) and DPPC (solid) at 37 °C. The total amount of vesicle lipid was 0.025 μmol (50 μM), and the large vesicle fractions were used. Points ▲ and △ (and ● and ○) refer to experiments without and with cytochalasin B (2 μg/mL) with DPPC (and with DMPC). Points designated ⊤ and ⊥ refer to theoretical calculations described in the text, using values for the parameters given in Table II.

Table I: Calculated Surface Densities of Antibodies

calcd antibodies/ exposed haptens[a]	calcd IgG antibody density[b] (antibodies/μm^2)	calcd antibodies/ vesicle[d]
1:3125	5.33 (8.0)[c]	16.7
1:625	26.7 (40.0)	83.8
1:125	133.0 (200)	419.0
1:25	667.0 (1000)	2094.0
1:5	3330 (5000)	10470
1:1	16670 (25000)	52400

[a] Exposed lipid haptens in these vesicles are estimated to be 30% of the total lipid hapten present (Esser et al., 1979); this determination is based on an application of the chemical method of Schwartz & McConnell (1978). [b] Antibody densities are based on an assumed area per lipid molecule of 60 Å^2. [c] Numbers in parentheses give calculated antibody densities for solid phase lipids, but these numbers are not used for subsequent calculations in the text. The numbers in parentheses are larger because the two-dimensional surface areas of solid lipids are smaller. See Discussion. [d] Vesicles were assumed to have diameters of 1 μm based in part on freeze-fracture electron microscopy and also optical microscopy.

Figure 2 gives two comparison fluorescence photographs following washing of the cells and vesicles. We have not eliminated the possibility that this differential behavior is due to cytochalasin B remaining associated with DMPC but not DPPC. Note that the effects of cytochalasin B on phagocytosis depend both on the macrophage cell line and on the object being phagocytized (Ito et al., 1979).

When antibody-coated vesicles were mixed with macrophages and examined under the fluorescence microscope, there was no apparent difference in the degree of vesicle–vesicle aggregation of DMPC and DPPC at the 1:25 antibody/exposed hapten ratio. In the presence of cytochalasin B (to prevent phagocytosis), DMPC hapten-sensitized vesicles in the presence of specific antibody (1:25 antibody/exposed hapten ratio) were essentially uniformly distributed close to the plasma membrane of the macrophage and showed no evidence of antibody-induced vesicle aggregation. During a 1-h incubation, all observed binding and/or phagocytosis was strictly antibody dependent, since no binding was detectable in the absence of antibody (see Figure 1). The lack of any antibody-independent binding in 1 h is probably due to the rapid swirling of the macrophages and vesicles in the incubation chamber, since

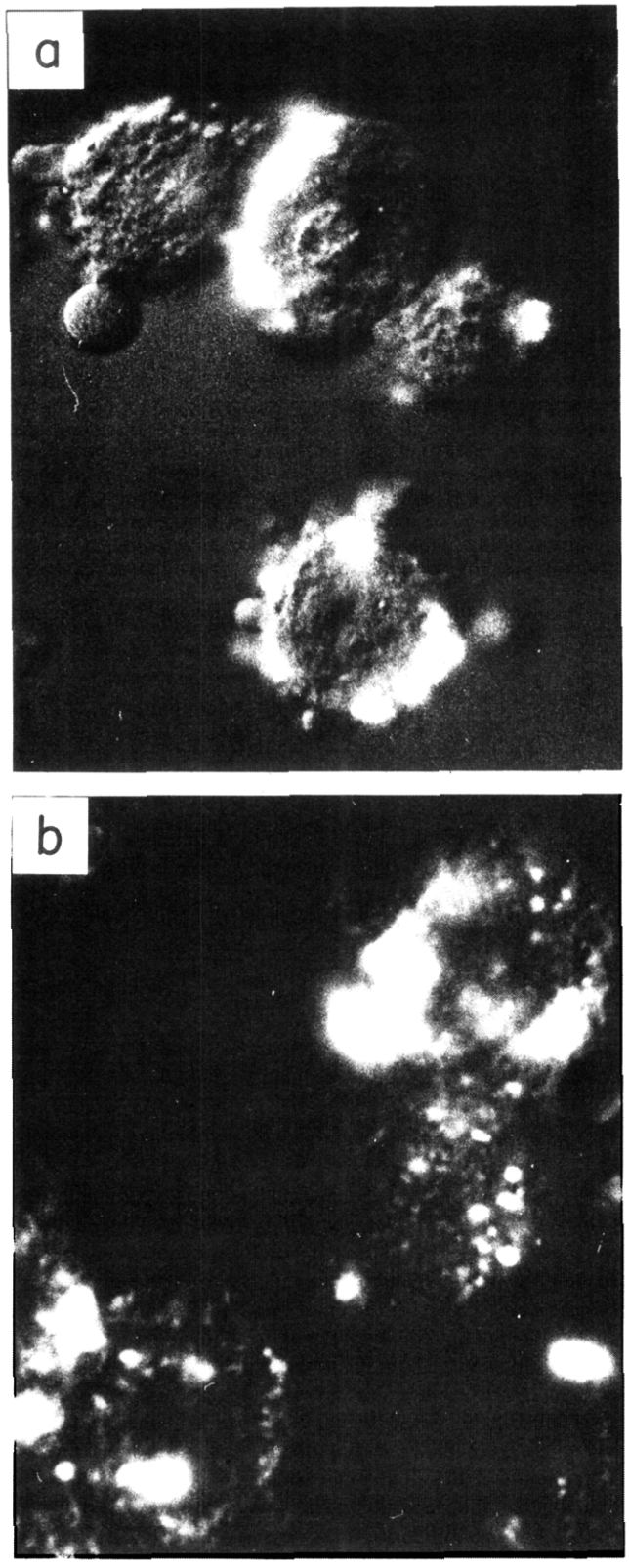

FIGURE 2: Fluorescence microscope photographs of RAW264 macrophages after treatment with 2 μg/mL cytochalasin B and specific antibody-coated lipid hapten sensitized vesicles composed of DMPC (a) and DPPC (b), prepared under conditions described in the text. The antibody/exposed hapten ratio is 1:25. The large vesicle fractions were used. The purpose of the photographs is to demonstrate that under these experimental conditions the vesicles show a specific antibody-dependent binding to the macrophage surface, but there is only observable phagocytosis in the case of the smaller of the DPPC vesicles (b).

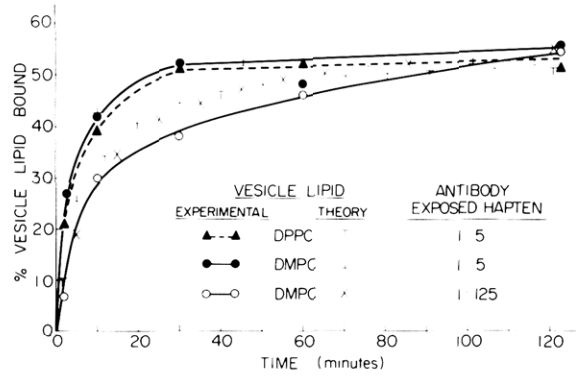

FIGURE 3: Kinetics of the specific antibody-dependent binding of lipid hapten sensitized lipid vesicles to RAW264 macrophages. The total amount of vesicle lipid is 0.025 μmol, and the medium-size fractions of the vesicles were used. ▲, ●, and O refer to DPPC, DMPC, and DMPC vesicles with antibody/exposed hapten ratios of 1:5, 1:5, and 1:125. Points designated ⊤, ⊥, and × refer to calculations for DPPC, DMPC, and DMPC with antibody/exposed hapten ratios of 1:5, 1:5, and 1:125, using values for the parameters equal to those in Table II except for k_0, λ_0, and ϵ which are 0.06, 6.90, and 2.07.

antibody-independent binding and phagocytosis have been observed when large liposomes are allowed to settle on macrophage monolayers (results not shown). The minimum antibody/exposed hapten ratio required to produce detectable binding (and phagocytosis) of hapten-containing DMPC vesicles was found to be 1:3125. The minimum antibody/exposed hapten ratio required to produce detectable binding (and/or phagocytosis) of hapten-containing DPPC vesicles was found to be fivefold higher (1:625) (see Figure 1).

In all experiments, there was no significant antibody-dependent binding of hapten-containing vesicles to macrophages at 0 °C. This was true even if the macrophages and antibody-coated vesicles were rapidly swirled.

Kinetics of Vesicle Binding. At high antibody density, the *rate* at which phospholipid becomes associated with macrophages does not depend strongly on phospholipid composition. Figure 3 illustrates that the kinetics of binding (and subsequent rapid phagocytosis) of DPPC vesicles at 1:5 antibody/exposed hapten ratio or DMPC at 1:5 and 1:125 antibody/exposed hapten ratios are very similar. It will be noted that the results presented in Figures 1 and 3 are similar but not identical (at the 1-h time point). It is possible that these differences are simply experimental error or are due to real differences in the vesicle or cell preparations. As will be discussed later, our interpretation of these kinetic data make it understandable that small variations in experimental conditions can lead to large changes in observed binding kinetics.

At lower antibody densities, however, DPPC vesicles become associated with macrophages at a much lower rate than DMPC vesicles. Figure 4 shows the rate at which hapten-containing vesicles of various phospholipid compositions become associated with macrophages at an antibody/exposed hapten ratio of 1:400. The addition of cholesterol to the DPPC vesicle membrane enhanced the binding to a value comparable to the DMPC vesicles. The addition of cholesterol to DMPC vesicles produced no significant effect on the binding rate.

Experimentally, the binding rate is determined by measuring the amount of a ^{14}C marker phospholipid which becomes associated with the macrophages. This binding rate is slow compared to the ~3 min needed for phagocytosis of a bound DMPC vesicle, as estimated by optical microscopy, for an antibody/exposed hapten ratio of 1:400. Under these conditions, the experimentally determined "binding rate" appears to be limited by the number of vesicle–cell collisions per unit

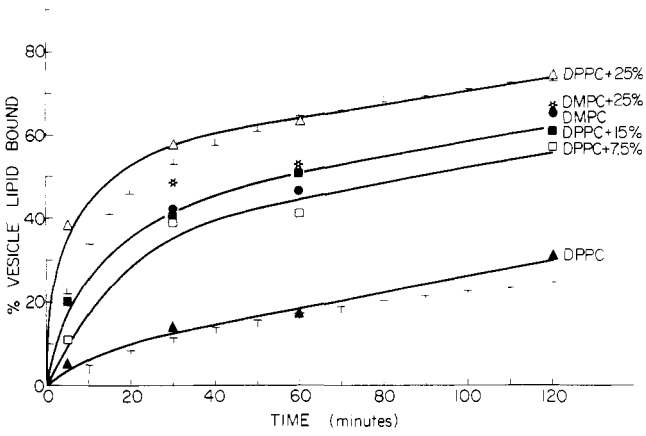

FIGURE 4: Effects of vesicle cholesterol on the kinetics of specific antibody-dependent binding of lipid hapten sensitized lipid vesicles to RAW264 macrophages. The total amount of vesicle lipid is 0.020 μmol, and the medium-size fractions of the vesicles were used. The symbols ▲, □, ■, and △ refer to DPPC vesicles containing 0, 7.5, 15, and 25 mol % cholesterol. The symbols ● and * refer to DMPC vesicles containing 0 and 25 mol % cholesterol. The antibody/exposed hapten ratio is 1:400. Points designated ⊤ and ⊥ refer to theoretical calculations for DPPC and DMPC, without cholesterol, using the parameters given in Table II.

time which result in adhesion rather than the rate of phagocytosis. Hence the experimentally determined rate is called a binding rate. At high antibody/exposed hapten ratios, the phagocytic rate increases markedly, being <1 s for an antibody/exposed hapten ratio of 1:5 for DPPC.

It is seen in Figure 4 that after 60 min, there is a low linear rate of vesicle binding independent of the lipid composition. This might be due in part to antibody-independent binding which results after the macrophages begin to attach to the walls of the incubation vessel. No antibody-independent binding is detected before 1 h, but as much as 30% binding has been observed after 3 h of incubation at 37 °C. As discussed later, we believe that the decrease in the initial binding rate, which is most obvious after 30 min, is related to receptor depletion.

The ordering of binding rates as a function of cholesterol content of the vesicles shows some variation from experiment to experiment. In the kinetic experiments shown in Figure 5, the addition of cholesterol to the DPPC vesicles results in a steady increase in the binding rate at short times, such that DPPC vesicles with 50 mol % cholesterol bind at the rate of pure DMPC vesicles, or at an even higher rate. This result is different from that shown in Figure 4, where 25 mol % cholesterol in DPPC shows the maximum binding rate. Also, in Figure 4 the binding rates of DPPC with 7.5 or 15 mol % (or 50 mol %, not shown) cholesterol and the binding rates of DMPC with or without 25 mol % cholesterol are similar, in contrast to the spectrum of different binding rates shown in Figure 5. The cause of these discrepancies is unknown at present.

Analysis of Binding Kinetics

The kinetics of vesicle binding illustrated in Figures 3–5 have a distinctly non-first-order time dependence. Moreover, in all cases the fraction of vesicles that are bound and/or phagocytized by the macrophages at long times is <100% of those available. Therefore, some factor other than exhaustion of the vesicle concentration must limit the binding rate. We suggest that depletion of receptors by phagocytosis or masking by membrane-associated vesicles is the limiting factor. A study of antibody-dependent loss of Fc receptors during phagocytosis

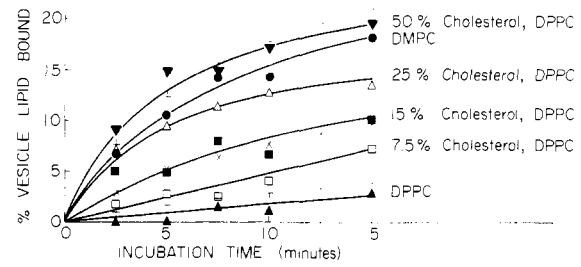

FIGURE 5: Early kinetics of specific antibody-dependent binding of lipid hapten sensitized lipid vesicles to RAW264 macrophages, as a function of lipid composition of the vesicles. The total amount of vesicle lipid is 0.020 μmol, and the medium-sized fraction was used. The antibody/exposed hapten ratio was 1:400. Points ▲, □, ■, △, and ▼ refer to DPPC vesicles containing 0, 7.5, 15, 25, and 50 mol % cholesterol. The points ● refer to DMPC vesicles. Points designated ⊤, ×, and ⊥ refer to calculations for DPPC vesicles containing 0 and 20 mol % cholesterol and for DMPC vesicles. The calculations employed the parameters given in Table II except for k_0, λ_0, and ϵ which are 0.06, 9.66, and 2.41. The unusually large values for λ_0 and ϵ required to fit these data may be related to inefficient ^{14}C-labeled lipid extraction from the macrophage (see Materials and Methods).

has been reported by Schmidt & Douglas (1972). A recent study of inhibition of antibody-dependent rosetting of sheep red blood cells following antibody-dependent phagocytosis of haptenated vesicles by RAW264 macrophages also indicates loss of Fc receptors (Petty et al., 1980). An important question for the present study is the relationship between the loss of receptors and the loss of free vesicles. Two simple possibilities are reasonable a priori. (a) The number of Fc receptors internalized by a vesicle is equal to or proportional to the number of antibodies on the vesicle surface. (b) The number of Fc receptors lost when a vesicle is internalized is some fixed number, independent of the antibody density when the antibody density is above some lower critical value. The kinetic analysis of our results provides evidence that neither of these possibilities is consistent with our data.

The problem of the relationship between the stoichiometry of receptor depletion and vesicle uptake can be formulated as follows. The rate of loss of vesicles from solution can be represented by the general equation

$$dV/dt = -k_0 V F(R,A) \quad (1)$$

Here V is the number of free vesicles per unit volume, and $k_0 V$ is the number of collisions per minute between free vesicles and macrophages. R is density of Fc receptors on the macrophage membrane which are available to bind antibody, and A is the density of antibodies on the hapten-containing lipid vesicle. Note that this expression for the collision rate is an assumption, since the collisions between macrophages and vesicles are brought about by stirring (a theoretical diffusion-limited rate constant, $\simeq 5 \times 10^{-3}$ min^{-1}, is much smaller than the values of k_0, $\simeq 0.1$ min^{-1}, derived later from the experimental data). The expression $F(R,A)$ is the fraction of the collisions that lead to binding. We have considered three models leading to different expressions for $F(R,A)$. In two of the simpler models, $F(R,A)$ is expressed as a product of a function of R and a function of A.

$$F(R,A) = \rho(R)\alpha(A) \quad (2)$$

If we make assumption a above, the total loss of receptors per unit volume is

$$\Sigma \delta R \simeq A \sigma \delta V \quad (3)$$

where Σ is the macrophage surface area per unit volume, σ is the effective surface area of a lipid vesicle as discussed later, A is the antibody surface density, and δR is the variational change in the receptor surface density of a macrophage re-

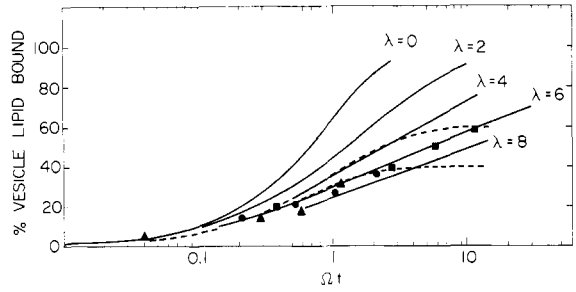

FIGURE 6: The fraction of vesicles bound to macrophages as a function of Ωt and λ, where Ω is the rate constant defined in eq 9 and λ is the receptor depletion parameter given in eq 10. Data points indicated by ●, ■, and ▲ refer to experimental kinetic binding data (from Figure 4) using vesicles of DMPC, DPPC with 15 mol % cholesterol, and pure DPPC. The corresponding values of Ω that best fit the data are $\Omega = 0.054$, 0.095, and 0.01 min^{-1}, respectively. Values for Ω for DPPC containing 25 and 50 mol % cholesterol were 0.35 and 0.08 min^{-1}, respectively. The antibody/exposed hapten ratio is 1:400 in all cases. The data for DMPC were taken on a different day; the value for Ω for DMPC taken on the same day as the other data in this figure is $\Omega = 0.1$ min^{-1}, and λ remains equal to 6. Also given in this figure are calculated binding curves corresponding to a second-order reaction rate mechanism based on the stoichiometric relations of eq 4 and 7 employing parameters equivalent to $\lambda = 1.67$ (upper dashed curve) and $\lambda = 2.5$ (lower dashed curve). For these dashed curves Ωt is $^2/_3$ the value given on the horizontal axis. These theoretical curves were positioned so as best to fit the experimental data.

sulting from a variational change δV in the free vesicle concentration due to vesicle uptake. For assumption b above the relation between δR and δV is

$$\Sigma\delta R = R_0\sigma\delta V \tag{4}$$

A third possibility is that the variation in receptor depletion, δR, with variation in vesicle concentration, δV, is proportional to $R(t)$ itself rather than R_0, the initial receptor density at time $t = 0$. This could arise if the macrophage quickly replaces plasma membrane lipid lost during phagocytosis but not receptors. In this case

$$\Sigma\delta R = R\sigma\delta V \tag{5}$$

Equations 3–5 can be regarded as operational definitions for σ, but in all cases it is presumed that σ has a value on the order of magnitude of the surface area of a vesicle. The integrated forms of eq 3–5 are

$$R = R_0 - (\sigma A/\Sigma)(V_0 - V) \tag{6}$$

$$R = R_0 - (\sigma R_0/\Sigma)(V_0 - V) \tag{7}$$

$$R = R_0 \exp[-(\sigma/\Sigma)(V_0 - V)] \tag{8}$$

As discussed below, we have eliminated the stoichiometic relations given in eq 6 and 7 based on a comparison between observed and calculated vesicle binding curves, when $\rho(R)$ is taken to be proportional to R. This essentially means that the disappearance of vesicles and receptors cannot be treated as a simple second-order reaction. Also, it will be seen that the disappearance of vesicles cannot be treated as a pseudo-first-order reaction.

We now show the plausibility of the stoichiometric relation, eq 8. When the expression for $R(t)$ from eq 8 is substituted into the differential equation eq 1, assuming the separability of $F(R,A)$ as in eq 2, and $\rho(R)$ is assumed to be proportional to R, $\rho(R) = R\rho_0$, the equation can be integrated to yield

$$\exp[\sigma V_0/\Sigma]\int_V^{V_0} \frac{\exp[-\sigma V/\Sigma]}{V}\,dV = \Omega t \tag{9}$$

Here $\Omega = k_0 R_0 \rho_0 \alpha(A)$.

The results of this integration are plotted in Figure 6. The left-hand member of the equation was evaluated for various values of the lower limit V, corresponding to various values of the percent vesicle uptake, and for various values of λ, where

$$\lambda = \sigma V_0/\Sigma \tag{10}$$

Thus defined, λ is the initial total surface area of lipid vesicles that is effective in depleting macrophage receptors divided by the total macrophage surface area. The percent vesicle uptake was plotted as a function of the log of the value of the left-hand member of eq 9, for various values of λ. Experimental data (from Figure 4) were then plotted on separate paper as percent vesicle uptake vs. log t. The two plots on the two sheets of paper were then shifted laterally until the experimental and theoretical curves matched within reasonable limits. Such comparisons showed that for vesicles with antibody/exposed hapten ratios of 1:400, all the data fall reasonably well on the theoretical curves for λ between 6 and 8 and for various values of Ω, as illustrated in Figure 6. The values of Ω ranged from 0.01 (DPPC) to 0.35 min^{-1} (DPPC containing 25 mol % cholesterol). These results strongly support the validity of the stoichiometric relation in eq 5 and 8. The shapes of the solid theoretical curves in Figure 6 are not changed if $\rho(R)$ is proportional to some power of R; for example, if $\rho(R)$ were proportional to R^2, the solid curves in Figure 6 would be labeled $\lambda = 0$, 1, 2, 3, and 4. Note that $\lambda = 0$ corresponds to a pseudo-first-order loss of vesicles; pseudo-first-order kinetics cannot possibly account for the experimental data. Note also that Figure 6 contains an illustrative calculation using eq 6 and 7 based on the second-order kinetic stoichiometric relations eq 3 and 4 (which are equivalent for fixed values of A). These calculated results are at variance with much of the experimental data in that they show a rather sharp break in vesicle uptake rate near the end of the reaction. The validity of the stoichiometric relation, eq 5 and 8, together with the kinetic analysis, implies a receptor redistribution and dilution by inserted lipid that is rapid compared to the uptake rate. It is likely that the stoichiometric relation of eq 5 and 8 *is* correct. It is also likely that the assumptions that $F(R,A)$ is separable (eq 2) and that $\rho(R)$ is simply proportional to R are oversimplifications. We have therefore considered a more detailed model but one that retains the stoichiometry of eq 5 and 8.

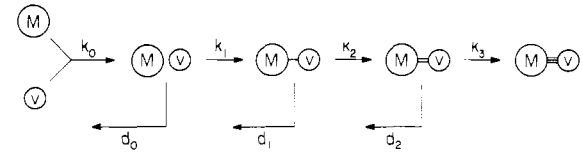

FIGURE 7: Detailed kinetic model for antibody-dependent binding of antibody-coated vesicles (V) to macrophages (M). Four stages of macrophage–vesicle association are shown, having 0, 1, 2, and 3 Fc–Fc receptor bonds; k_0, k_1, k_2, k_3, d_0, d_1, and d_2 are kinetic parameters (see text for details).

Figure 7 depicts hypothetical successive steps of Fc–Fc receptor bond formation and dissociation for macrophage–vesicle associations that have zero, one, or two bonds. It is assumed that if three bonds are formed, the association is permanent (additional bonds may be formed after the third). Note that the kinetic scheme depicted in Figure 7 is not a conventional scheme such as one might write for a sequence of chemical reactions. In other words, the back-reactions corresponding to k_1, k_2, and k_3 have been omitted. This is based on our assumption that vesicles are more likely to be hydrodynamically stripped from the macrophage in the one-step dissociation process given by the rates d_0, d_1, and d_2 before the back-reactions can occur. Each of these dissociation steps yields a free vesicle.

Table II: Kinetic Parameters[a]

$k_0 = 0.10\ \text{min}^{-1}$
$k_{1i} = 606\ \mu\text{m}^4/\text{min}$
$k_{2i} = 90\ \mu\text{m}^4/\text{min}$
$k_{3i} = 0$
$4DS$[b] $= 1920\ \mu\text{m}^4/\text{min}$ for DMPC; $4DS = 2.4\ \mu\text{m}^4/\text{min}$ for DPPC
$d_0 = 6.0 \times 10^6\ \text{min}^{-1}$
$d_1 = 4.0 \times 10^6\ \text{min}^{-1}$
$d_2 = 4.0 \times 10^3\ \text{min}^{-1}$
$\lambda = \lambda_0 + \epsilon[1 - \exp(-A/A_s)]$ if $A > R$
$\lambda = \lambda_0$ if $A < R$
$A_s = 333\ \mu\text{m}^{-2}$
$\lambda_0 = 3.68$ for 0.02 μmol of lipid; $\lambda_0 = 4.60$ for 0.025 μmol of lipid
$\epsilon = 0.83$ for 0.02 μmol of lipid; $\epsilon = 1.03$ for 0.025 μmol of lipid

[a] These kinetic parameters are based on the assumption that each macrophage has 2×10^5 Fc receptors for rabbit antibody and that the macrophage has a surface area of 1000 μm^2. The estimated initial number of vesicles for each experiment is 6.9×10^8 for 0.02 μmol of lipid and 8.6×10^8 for 0.025 μmol of lipid. Vesicles are assumed to have a diameter of 1 μm, and the lipids have an area of 60 Å^2. All parameters are assumed to be the same for fluid and solid lipid vesicles, except for the terms proportional to the diffusion coefficients. [b] $S = 1\ \mu\text{m}^2$.

We have further assumed that the bond-forming rate constants have the forms

$$k_1 = RA[k_{1i} + 4DS] \quad (11)$$

$$k_2 = [(RS - 1)/S][(AS - 1)/S][k_{2i} + 4DS] \quad (12)$$

$$k_3 = [(RS - 2)/S][(AS - 2)/S][k_{3i} + 4DS] \quad (13)$$

In these equations R and A are surface densities of macrophage receptors and vesicle-bound antibodies, respectively; S is the area of the macrophage membrane which is in contact with a single bound vesicle; D is the lateral diffusion coefficient of antibodies bound to the vesicle surface; and k_{1i}, k_{2i}, and k_{3i} are parameters which describe the "antibody diffusion independent" bond formation processes which are discussed later. The values for the parameters used in fitting the kinetic data are shown in Table II.

This model allows for the possibility that the first and second bond formation steps may occur by two mechanisms, one of which requires that an antibody on the vesicle diffuses *in the plane of the vesicle membrane* to an Fc receptor on the macrophage while the macrophage and vesicle are in contact. This process will be termed the "antibody diffusion dependent" mechanism. The other mechanism which can operate concurrently with the first but is independent of molecular lipid diffusion involves rapid local relative motions between the macrophage and vesicle which can bring antibodies and receptors together. Equations 11 and 12 assume random distributions of antibodies and receptors in the macrophage–vesicle contact region where Fc–Fc receptor bonds are formed, and, therefore, k_1, k_2, and k_3 are proportional to the product of the number of free receptors and antibodies in the contact region.

The first and second bond formation steps can occur by antibody diffusion on the vesicle membrane as well as by relative motions of vesicle and macrophage. It is assumed that the third bond formation step occurs only by the antibody diffusion dependent mechanism. In other words, $k_{3i} = 0$ in eq 13. In making this latter assumption, it would appear that we have neglected receptor diffusion, which would be significant if the receptor diffusion constant were larger than 10^{-10} cm^2/s. This point is discussed later.

We shall use the terminology "antibody diffusion independent" reaction mechanisms to include all molecular motions that bring receptors and antibodies together, other than those that involve lateral diffusion of bound antibodies in the plane of the vesicle membrane. Some of these antibody diffusion independent processes might involve translational and rotational diffusion of the vesicle, but, as will be discussed later, the large values of the parameters used to describe the antibody diffusion independent reaction mechanisms suggest that factors other than vesicle diffusion are required to account for the large rates of these processes.

The diffusion-dependent mechanism of antibody–receptor bond formation presents a potentially difficult analytical problem because of the two-dimensional character of the diffusion. In two dimensions there is no time-independent diffusion-limited steady-state rate constant [see, for example, Razi-Naqvi (1974)]. Since we are only interested in the initial capture rate, a simple lattice calculation can be used to obtain this rate. This rate constant k_d is

$$k_d = 4DRAS \quad (14)$$

where D is the diffusion constant of antibodies bound to lipid haptens. This equation is derived in the Appendix. A rate constant approximately equal to that given in eq 14 has been employed by Bell (1978, 1979) in calculations of receptor–ligand bond formation between two cell surfaces. Our values for D have been taken equal to the diffusion constants for the vesicle lipids, since antibodies bound to lipid haptens move as rapidly as the lipids themselves (Smith et al., 1979).

Combining the antibody diffusion independent and diffusion dependent mechanisms gives the capture rates shown in eq 11–13. Corresponding to the six first-order rate constants, there are four first-order coupled linear differential equations involving the instantaneous concentration of vesicles and macrophages and vesicle–macrophage complexes having 0, 1, 2, or 3 bonds.

In the course of fitting the various kinetic experiments to empirical values of these parameters, we have found by direct computation that the usual steady-state approximation for the reaction intermediates (complexes with 0–2 bonds) is valid. With this steady-state approximation for the intermediates, we obtain the expression eq 15 for the fraction of successful collisions, $F(R,A)$, used in eq 1. A comparison of this expression and eq 11–13 illustrates that $F(R,A)$ is not separable, in general, as in eq 2.

$$F(R,A) = 1 - \frac{d_0}{d_0 + k_1} - \frac{d_1 k_1}{(d_1 + k_2)(d_0 + k_1)} - \frac{d_2 k_2 k_1}{(d_2 + k_3)(d_1 + k_2)(d_0 + k_1)} = \left(\frac{k_1}{d_0 + k_1}\right)\left(\frac{k_2}{d_1 + k_2}\right)\left(\frac{k_3}{d_2 + k_3}\right) \quad (15)$$

Values for the parameters that have been used in fitting all of the experimental data are given in Table II, except for values of k_0 and λ. Variations of k_0 in the range 0.06–0.10 min^{-1} were required to fit various kinetic data, as indicated in the figure legends. Values of the parameters shown in Table II were chosen by the following protocol: since (1) increasing antibody concentrations do not increase the rate of vesicle binding once a critical surface density is exceeded and (2) the rates of vesicle binding, as the antibody density is increased above ~666 antibodies/μm^2 (1:25 antibody/exposed hapten ratio), become nearly independent of lipid composition, at early reaction times and high antibody surface density, the fraction of successful collisions, $F(R,A)$ (eq 1 and 15), would be expected to approach unity. In other words, under these conditions, the rate of vesicle binding is evidently limited by the rate of collisions. In this case the shape of the binding curve is determined by k_0 and λ. The initial binding rate is then $k_0 V$,

so that k_0 is determined by the early time points of the experimental kinetic binding curves at high antibody surface densities. The relatively sharp asymptotic behavior seen in the binding of vesicles at high antibody densities (Figure 3) determines the appropriate parametric value of λ, typical values of which are in the range 3.7–9.7. That is, at long times (e.g., 1 h) the percentage of vesicles bound determines the value of the parameter λ. As will be discussed later, values of λ at high antibody densities are larger than those at low antibody density by ~20%. λ is certainly not proportional to the antibody density.

The determinations of the various parameters for low antibody densities are more intricate but are far from arbitrary. The considerations determining the choice of parameters are listed as follows: (1) values of Ω estimated by using the method of eq 9 and Figure 6 and the experimental data shown in Figure 1 show that the binding rate is approximately quadratic in the antibody density for DMPC at low antibody densities. This fact, coupled with the relative binding of DMPC and DPPC at the 1:625 antibody/exposed hapten ratio along with our placing of a plausible upper limit on the rates of the antibody diffusion independent processes, places severe constraints on the values of the dissociation rates d_0, d_1, and d_2. The dissociation rate d_2 is then forced by the experimentally observed DPPC binding rates to be small, since the formation of the third antibody–receptor bond is assumed to occur only by the diffusion-dependent process. Given a small d_2, the experimental quadratic dependence of Ω on A requires that $d_0 > k_1$ and $d_1 > k_2$. This can be seen from eq 15. Therefore, if an upper limit is imposed on the antibody diffusion independent rates contained in k_1 and k_2, all of the remaining parameter values are determined uniquely by features of the experimental data.

In general, slightly larger values of λ were required to fit the experimental data at high antibody densities than were required at low antibody densities. It can be postulated that the physical basis for this effect is related to the relative magnitudes of the antibody density on the vesicle surface and the receptor density on the macrophage surface. That is, when the antibody density exceeds the receptor density, additional receptors are apparently depleted. We have employed eq 16 in our computer program to simulate this dependence of λ on antibody density. This particular form can be regarded as

$$\lambda = \lambda_0 + \epsilon[1 - \exp(-A/A_s)] \text{ if } A > R$$
$$\lambda = \lambda_0 \text{ if } A \leq R \qquad (16)$$

a computational convenience; A_s characterizes the antibody density above which further increases in antibody density do not result in further depletion of receptors per veiscle bound. This is particularly important for the case of 1:125 antibody/exposed hapten ratio for DMPC in Figures 1 and 3, where, during the course of the kinetic curve, $A \leq R$ applies for short times and $A > R$ applies for long times. This form assumes that the efficiency of capture of extra receptors when $A > R$ is linear in the antibody density for small A but quickly approaches some upper limit measured by ϵ, which is 22–30% of λ_0. Comparisons between calculations and experimental data are given in Figures 1, 3, 4, and 5.

Discussion

We have measured the specific antibody-dependent binding of haptenated vesicles to macrophages as a function of vesicle lipid composition. A number of conclusions can be drawn from a qualitative examination of the data.

At low antibody densities, the binding kinetics are strongly vesicle lipid dependent, whereas at high antibody densities the binding kinetics are relatively independent of vesicle lipid composition (see, for example, Figures 1, 4, and 5). This observation is consistent with the idea that lateral diffusion of bound antibodies is important for binding and/or phagocytosis at low antibody densities. Under the experimental conditions of Figure 1, the lateral diffusion coefficients of hapten-bound rabbit IgG antibodies are estimated to be 10^{-10} cm^2/s for DPPC vesicles and 8×10^{-8} cm^2/s for DMPC vesicles (Rubenstein et al., 1979; Smith et al., 1979). Of course one cannot rule out the possibility that vesicle membrane flexibility also plays a role in the enhanced binding of DMPC vesicles relative to DPPC vesicles. It will be noted in Figures 4 and 5 that the inclusion of a small concentration of cholesterol (7.5 mol %) in DPPC vesicles has a marked effect in enhancing the rate of the vesicle binding to macrophages. From other work it is known that at 37 °C the inclusion of this concentration of cholesterol produces parallel, ordered domains of fluid and solid lipid, the solid domains being pure DPPC (Copeland & McConnell, 1980; Owicki & McConnell, 1980). If lateral diffusion of bound antibodies does limit the rate of binding of DPPC vesicles to macrophages, the enhancement of this rate by low cholesterol content is readily understood. Note that the addition of cholesterol to fluid DMPC [which has only a minor effect on lateral diffusion of the lipid haptens (Rubenstein et al., 1979)] has no significant effect on the rate of vesicle binding to macrophages.

In one experiment, not described here in detail, the binding rates of vesicles of widely differing sizes (~0.1–1-μm diameter based on sedimentation velocities) were compared. It was found that the small vesicles did not bind as well as the large vesicles. This effect cannot be responsible for the differences in DMPC and DPPC vesicle binding reported here since these vesicle populations were selected to have similar sizes. On the other hand, the inclusion of cholesterol in DPPC vesicles has a pronounced effect on bilayer density, and this makes difficult the selection of vesicles on the basis of size by differential sedimentation. Thus, there is some uncertainty concerning the vesicle sizes for DPPC–cholesterol mixtures, although they do have sizes similar to the 1-μm DPPC vesicles used in most of our experiments. In any event, some caution is required in this respect in analyzing the cholesterol effects depicted in Figures 4 and 5.

We have attempted a quantitative analysis of the vesicle binding kinetics, as described in the preceding section. This study has led us to the conclusion that macrophage Fc receptors are depleted at an exponentially decreasing rate following binding of successive antibody-coated vesicles. It thus appears that receptors are lost due to phagocytosis of vesicles and that there is a continuous redistribution of receptors on the macrophage surface, such that the vesicles binding to the macrophage at later times result in the depletion of a smaller number of receptors per vesicle. This vesicle–receptor stoichiometric relation is expressed in eq 5 and is manifest experimentally in the shape of the kinetic binding curves. The conformance of some of the experimental data to this stoichiometry is illustrated in Figure 6.

The schematic, detailed kinetic model depicted in Figure 7 is the simplest model that we have been able to devise that is consistent with all of our kinetic data. In addition to incorporating the stoichiometric relation just discussed (eq 5), the model gives a quantitative expression for $F(R,A)$, the fraction of successful collisions (cf. eq 15). In this model, for the parameters given in Table II, the large differences in the rate of DMPC vs. DPPC vesicle binding arise in the larger antibody diffusion dependent rate for DMPC relative to DPPC

in all steps, and especially the last step—the antibody diffusion dependent formation of the third Fc–Fc receptor bond. The values of the parameters d_0, d_1, d_2, k_1, k_2, and k_3 determine the dependence of the vesicle binding rate on antibody concentration as illustrated by the data in Figure 1. As mentioned earlier, this experimentally observed binding rate is quadratic in the antibody concentration when this concentration is very low, and this is accounted for by eq 15 if d_2 is small, $d_0 \gg k_1$, and $d_1 \gg k_2$. Since k_1 and k_2 are very nearly proportional to the antibody density, the initial binding rate will become linear in A for intermediate antibody densities (antibody/exposed hapten = 1:400; cf. eq 2 and 9 and Figure 6) and independent of A for high antibody densities. [In a similar way, $F(R,A)$ can show a complex and exponential dependence on the antibody diffusion constant D.] This argument is also true with respect to the receptor density, R, since the fraction of successful collisions, $F(R,A)$ (eq 15), is symmetric in R and A.

The mathematical form $F(R,A)$ includes the possibility of receptor diffusion, in that the diffusion coefficient D in eq 11–13 could be regarded as a *mutual* receptor–antibody diffusion coefficient, rather than the antibody diffusion coefficient itself. Thus we have neglected the receptor diffusion in the selection of parameter values only in the sense that we have assumed it to be small compared to antibody diffusion on DMPC and DPPC vesicles. It has been shown by computation that, if this latter approximation were not valid and the receptor diffusion were as high as 10^{-9} cm^2/s, there is, for example, only a 10% increase in the vesicle binding in 1 h when the antibody/exposed hapten ratio is 1:125.

An important question concerning our model is the extent to which the model parameters (Table II) are physically plausible. The pseudo-first-order rate constant $k_0 = 0.10$ min^{-1} given in Table II is $\sim$20 times larger than a theroretical (unstirred) diffusion-limited rate constant (5×10^{-3} min^{-1}); this is consistent with the fact that our system is hydrodynamically swirled. On the other hand, the observed rate constant k_0 is consistent with any mixing process which is limited by a diffusion step through a small distance, 0.5 μm. We feel that this value of k_0 in Table II is physically plausible.

The three ratios k_1/d_0, k_2/d_1, and k_3/d_2 determine $F(R,A)$ in eq 15. The absolute magnitudes of k_1, k_2, and k_3 are set by the known values of the diffusion coefficients D, the antibody density A, the estimated receptor density R, and the antibody independent diffusion parameters k_{1i}, k_{2i}, and k_{3i}. In our model these parameters have been included to represent all motions of vesicles relative to the macrophage that facilitate Fc–Fc receptor bond formation, except for lateral diffusion of antibodies in the plane of the vesicle membrane. The parameter k_{3i} is set equal to zero since it is plausible that with two Fc–Fc receptor bonds the vesicle is "anchored" so that the relative motions of vesicle and macrophage are inhibited to the extent that they cannot compete with antibody lateral diffusion in facilitating the formation of the third Fc–Fc receptor bond. The magnitudes of k_{1i} and k_{2i} are quite large and difficult to explain by using any simple molecular model. Perhaps the simplest general idea is that the macrophage membrane has a lateral inhomogeneity and that the vesicle first binds nonspecifically with a certain "sticking" free energy. If this sticking free energy has a gradient in some direction it is entirely possibile that the vesicle may translate and rotate over distances that are so large as to significantly increase the likelihood of Fc–Fc receptor bond formation. (We have observed rapid, 100–1000 μm/s displacements of fluorescent-labeled lipid vesicles over distances on the order of microns on clean glass surfaces in the absence of macrophages.) At the antibody/exposed hapten ratio of 1:625, where the binding of DPPC vesicles to macrophages is first detected (Figure 1), the average nearest lateral center to center distance between antibody (on the vesicle) and receptor (on the macrophage) is estimated to be only on the order of magnitude of 100–200 Å, assuming a receptor density of 200–400 μm^{-2} (Steinman et al., 1976; Segal & Hurwitz, 1977), so the distances over which rapid motions (parameterized by k_{1i} or k_{2i}) must take place are not large.

For given values of the parameters k_1, k_2, and k_3, the values of d_0, d_1, and d_2 are established, since $F(R,A)$ is a function of the ratios k_1/d_0, k_2/d_1, and k_3/d_2 and the form chosen for $F(R,A)$ is required to fit the experimental data. A priori, we have no way of estimating the orders of magnitude of d_0, d_1, and d_2. The low value of d_2 compared to d_0 and d_1 is consistent with the notion that two Fc–Fc receptor bonds stabilize the macrophage–vesicle complex compared to either one or no bonds. (In this model, three bonds are assumed to further stabilize the macrophage–vesicle complex to an extent sufficient to always allow the formation of whatever number of additional bonds are required for permanent binding.) In the following discussion of the uniqueness of this model, it is pointed out that these parameters need not represent true values of the rates at which vesicles leave the surface of the macrophage but instead only rigorously characterize the rates of processes which compete irreversibly with Fc–Fc receptor bond formation. That is, these processes result in a state such that a vesicle no longer participates in bond formation without first leaving the macrophage surface and joining the vesicles free in solution.

The experimental values for λ (Table II) have physically plausible orders of magnitude, in terms of the definition of λ given by eq 10. As discussed earlier in connection with eq 3–5, σ is expected to have a value on the same order as the vesicle surface area. The characteristic values of λ used for fitting the experimental data fall in a range such that σ in eq 10 is 1.7–4.5 times the calculated vesicle surface area. The effect of antibody density on the apparent value of λ is small, and from this we infer that large numbers of receptors do not move from afar to the region of vesicle binding and so become depleted.

Unfortunately, the number of Fc receptors which bind rabbit antibody have not been measured for the RAW264 cell line. For some macrophage cell lines which have similar properties, the number of receptors has been estimated by a Scatchard analysis of the binding of rabbit antibody trimers in solution (Segal & Hurwitz, 1977). However, the precise value for the initial number of receptors (or the initial receptor density) has no effect, in practice, on the fitting of the kinetic data to the model because any future correction in the initial receptor density given in Table II could always be absorbed in the parameters k_{1i}, k_{2i}, or S (eq 11–13). A similar argument is valid for variations in vesicle size, vesicle number, or macrophage surface area. Note that the difference in lateral lipid concentration between the solid phase and fluid phase lipids (cf. Table I) has been ignored in deriving the parameters in Table II. Such differences could also be incorporated with compensating small changes in the parameters k_{1i}, k_{2i}, or d_0.

An important question concerns the uniqueness of our model. In other words, (a) how many other models can account for the data, (b) with how many different physical pictures are our model parameters consistent, and (c) what latitude is there in the choice of the model parameters? In connection with question a, we have tried a number of other

models that have failed to account for the results. In particular, we have tried "catch and diffuse" models, in which a vesicle–macrophage "collision" results in one or more bonds by statistical geometrical overlap, followed by diffusion events that result in permanent binding. The one advantage of the model of Figure 7 that appears to make it successful is that it treats the antibody diffusion independent steps as kinetically competitive with the antibody diffusion dependent steps. Thus, the model considers the relative motions of vesicle and macrophage in bringing about Fc–Fc receptor bond formation in competition with antibody diffusion. The failure of our various (unpublished) catch and diffuse models implies that bond formation resulting from "one-hit" overlap of antibodies and receptors is an inadequate description of the antibody diffusion independent processes.

Question b above is particularly important. As pointed out above, a clear interpretation of the parameters k_{1i}, k_{2i}, k_{3i}, d_0, d_1, and d_2 has not been possible. Part of this difficulty may be a lack of uniqueness in the physical processes that these parameters represent. For example, Figure 7 suggests that every bound vesicle leaves the surface of the macrophage at a rate d_0, etc. This may not be the case. It is entirely plausible that the relative macrophage–vesicle motion is such that an antibody reaches the region of an Fc receptor and has the relative probabilities $k_1/(k_1 + d_0)$ of being caught and $d_0/(k_1 + d_0)$ of not being caught by the Fc receptor. If a first antibody is not caught, the vesicle might move on to a steady-state pool of vesicles on the macrophage surface devoid of Fc receptors, from which it dissociates with a first-order rate much less than d_0. Thus, the particular scheme in Figure 7 is only a subset of a larger class of models described by the equations used.

The third question (c) concerns the range of parameter variations that is consistent with the experimental data. The only significant parameter variations possible are upward variations in k_{1i} and k_{2i} and a compensating upward variation in d_0, d_1, and d_2. We have chosen values of k_{1i} and k_{2i} close to their lower bounds. For example, the k_{1i} term chosen for DMPC and DPPC is approximately one-third the value of the equivalent antibody-dependent diffusion term, $4DS$, for DMPC (see Table II). Of course there is also the possibility of changing parameter values if it is assumed that only some fraction of the surface of the macrophage contains Fc receptors.

The fact that the 1-h binding of DMPC to the macrophage (Figure 1) is not greatly changed by cytochalasin B indicates that this substance does not greatly affect the quantitative relation between receptor depletion and vesicle uptake. That is, since cytochalasin B inhibits phagocytosis, one might expect a different relation between receptor depletion and vesicle uptake (from solution) in the presence and absence of cytochalasin B. Thus, for bound vesicles, the receptor–vesicle association must be irreversible on the time scale of the experiments, irrespective of whether binding is followed by phagocytosis or not. We suspect that in the presence of cytochalasin B the vesicles and Fc receptors may move into, or just below, the macrophage membrane surface, but no further.

We feel that the principal strength of our model and the associated experiments is that they provide a convenient starting point for additional, more definitive experiments under conditions better suited to test models of macrophage–vesicle interactions. Studies of the type presented here are of particular interest in connection with comparisons of the activation of other components of the immune system. For example, in a study of the kinetics of the antibody-dependent activation of the first component of complement by hapten-sensitized lipid membranes, DMPC is found to be more efficient than DPPC, in a manner that also suggests that lateral lipid diffusion is rate controlling in the case of DPPC. Further quantitative comparisons of this sort should be fruitful.

Acknowledgments

We are most grateful to Dr. Peter Ralph for his gift of the RAW264 cell line and to Drs. Peter Ralph and William Clark for many helpful discussions.

Appendix

In the present work we have used a special approximation to calculate the rate at which antibodies are captured by receptors, due to lateral diffusion of the antibodies in the plane of the vesicle membrane. We assume a two-dimensional square lattice, and antibodies and receptors are placed on lattice sites in proportion to their relative surface concentrations. It is further assumed that at time $t = 0$ there is zero probability of there being any Fc–Fc receptor bonds. Let a receptor be located at $x = y = 0$ and neighboring lattice sites be located at $x = l$ and $-l$ when $y = 0$ and at $y = l$ and $-l$ when $x = 0$. Let p be the probability that an antibody molecule be found at $x = l$, $y = 0$ at time $t = 0$. Let τ^{-1} be the site to site jump rate constant in the x direction for the antibody. Then the average rate that antibodies on a given site next to a receptor jump onto the receptor is ${}^1/_2 p\tau^{-1}$. For the one-dimensional diffusion, the jump rate constant is related to the diffusion coefficient D by eq A1 (Davidson, 1962). Thus, the

$$2D = \tau^{-1}l^2 \qquad \text{(A1)}$$

probability that an antibody from any one of the four nearest neighbors will jump onto the receptor is $4\,{}^1/_2 p\tau^{-1}$ which is $4Dp/l^2$. The probability that a lattice site will be occupied by an antibody is $p = l^2A$. The number of receptors is RS. Thus the initial Fc–Fc receptor bond formation rate is $(4Dp/l^2)(l^2A)(RS) = 4DRAS$, which is the result given in eq 14.

The above calculation makes two important approximations. (a) The first approximation is that at time $t = 0$ when the vesicle–macrophage contact is first made, there is a negligible probability of having an Fc–Fc receptor bond. (b) During the course of the first three Fc–Fc receptor bond formations the antibody concentration gradients that are set up are negligible. Approximation a can be justified by noting that the antibody diffusion dependent Fc–Fc receptor bond formation rate, $4DRAS$, does not depend on the choice of the magnitude of the lattice spacing. If we take the lattice spacing to be small (e.g., 10 Å), then for most experiments the probability of having an Fc–Fc receptor bond at $t = 0$ is negligible. Approximation b is justified as long as the number of antibodies in the contact region is large compared to three. Under these conditions no significant concentration gradients are set up and the special mathematical problem of diffusion in two dimensions is avoided (see below). The approximation leading to the antibody diffusion dependent bond formation rate, eq 14, is the same as that used before for the calculation of diffusion coefficients from steady-state spin-label paramagnetic resonance spectra (Sackmann & Träuble, 1972; Devaux et al., 1973). An expression for receptor–ligand binding kinetics similar to but not identical with eq 14 has been given by Bell (1978, 1979).

When the number of antibodies in the contact region is not large compared to three, then Fc–Fc receptor bond formation leads to large (ensemble average) concentration gradients in the contact region, which should in principle be treated by

using time-dependent ensemble average solutions of the two-dimensional diffusion equation. [For relevant literature, see Razi-Naqvi (1974), Adam & Delbrück (1968), Galla et al. (1979), and Montroll (1969).] These more detailed calculations should be employed, for example, for antibody/exposed hapten ratios of 1:3125 ($\sim$5 antibodies/μm^2). We have found by numerical calculation that these exact treatments indicate that under such conditions of low antibody densities, eq 14 overestimates the Fc–Fc receptor bond formation rate by no more than a factor on the order of 2.

References

Adam, G., & Delbrück, M. (1968) in *Structural Chemistry and Molecular Biology* (Rich, A., & Davidson, N., Eds.) p 198, W. H. Freeman, San Francisco. CA.

Baram, P., Battisto, J. R., & Pierce, C. W., Eds. (1979) *Dev. Immunol. 4.*

Bell, G. I. (1978) *Science 200*, 618.

Bell, G. I. (1979) *Dev. Cell Biol. 4*, 371.

Brûlet, P., & McConnell, H. M. (1977) *Biochemistry 16*, 1209.

Copeland, B. R., & McConnel, H. M. (1980) *Biochim. Biophys. Acta 599*, 95.

Davidson, N. (1962) *Statistical Mechanics*, p 284, McGraw-Hill, New York.

Deamer, D., & Bangham, A. D. (1976) *Biochim. Biophys. Acta 443*, 629.

Devaux, P., Scandella, C. J., & McConnell, H. M. (1973) *J. Magn. Res. 9*, 474.

Esser, A. F., Bartholomew, R. M., Parce, J. W., & McConnell, H. M. (1979) *J. Biol. Chem. 254*, 1768.

Galla, H.-J., Hartmann, W., Theilen, U., & Sackmann, E. (1979) *J. Membr. Biol. 48*, 215.

Geiger, B., & Schreiber, A. D. (1979) *Clin. Exp. Immunol. 30*, 149.

Hafeman, D. G., Parce, J. W., & McConnell, H. M. (1979) *Biochem. Biophys. Res. Commun. 86*, 522.

Hafeman, D. G., Lewis, J. T., & McConnell, H. M. (1980) *Biochemistry* (following paper in this issue).

Henkart, P., & Blumenthal, R. (1975) *Proc. Natl. Acad. Sci. U.S.A. 72*, 2789.

Henry, N., Parce, J. W., & McConnell, H. M. (1978) *Proc. Natl. Acad. Sci. U.S.A. 75*, 3933.

Humphries, G. M. K., & McConnell, H. M. (1976) *Biophys. J. 16*, 275.

Humphries, G. M. K., & McConnell, H. M. (1979) *J. Immunol. 122*, 121.

Humphries, G. M. K., & McConnell, H. M. (1980) *Methods Exp. Phys.* (in press).

Ito, M., Ralph, P., & Moore, M. A. S. (1979) *Cell. Immunol. 46*, 48.

Lewis, J. T. (1980) Ph.D. Thesis, Stanford University, Stanford, CA.

Lewis, J. T., & McConnell, H. M. (1978) *Ann. N.Y. Acad. Sci. 308*, 124.

Montroll, E. W. (1969) *J. Math. Phys. (N.Y.) 10*, 753.

Owicki, J. C., & McConnell, H. M. (1980) *Biophys. J. 30*, 383.

Parce, J. W., McConnell, H. M., Bartholomew, R. M., & Esser, A. F. (1980) *Biochem. Biophys. Res. Commun. 93*, 235; *94*, 735 (errata).

Petty, H. R., Hafeman, D. G., & McConnell, H. M. (1980) *J. Immunol.* (in press).

Ralph, P. (1980) in *Mononuclear Phagocytes—Functional Aspects* (van Furth, R., Ed.) Vol. 3 of Leiden Conference, The Hague, Martinns Nijhoff (in press).

Ralph, P., & Nakoinz, I. (1977) *J. Immunol. 119*, 950.

Razi-Naqvi, K. (1974) *Chem. Phys. Lett. 28*, 280.

Rey, P., & McConnell, H. M. (1976) *Biochem. Biophys. Res. Commun. 73*, 248.

Rubenstein, J. L. R., Smith, B. A., & McConnell, H. M. (1979) *Proc. Natl. Acad. Sci. U.S.A. 76*, 15.

Sackmann, E., & Träuble, H. (1972) *J. Am. Chem. Soc. 94*, 4492.

Schmidt, M. E., & Douglas, S. D. (1972) *J. Immunol. 109*, 914.

Schwartz, M. A., & McConnell, H. M. (1978) *Biochemistry 17*, 837.

Segal, D. M., & Hurwitz, E. (1977) *J. Immunol. 118*, 1338.

Smith, L. M., Parce, J. W., Smith, B. A., & McConnell, H. M. (1979) *Proc. Natl. Acad. Sci. U.S.A. 76*, 4177.

Steinman, R. M., Brodie, S. E., & Cohn, Z. A. (1976) *J. Cell. Biol. 68*, 665.

Stossel, T. P. (1977) *Recept. Recognition, Ser. A 4*, 103.